



Kinetics Study and Degradation Pathway of Methyl Orange Photodegradation in The Presence of C-N-codoped TiO₂ Catalyst

Reza Audina Putri¹, Safni Safni^{1*}, Novesar Jamarun², Upita Septiani²

¹Laboratory of Applied Analytical-Chemistry, Department of Chemistry, Faculty of Mathematic and Natural Sciences, Andalas University, Padang 25163, Indonesia

²Laboratory of Material, Department of Chemistry, Faculty of Mathematic and Natural Sciences, Andalas University, Padang 25163, Indonesia

³Institute of Health and Environment, Seoul National University, Seoul 08826, Korea



This work investigated the photodegradation of azo dye, methyl orange, without and with the addition of C-N-codoped TiO₂ catalyst using a visible halogen-lamp as a light source. C-N-codoped TiO₂ was prepared by free-organic solvent peroxo sol-gel method. The effects of initial dye concentration, catalyst dosage, and pH solution on the photodegradation of methyl orange were studied. Photodegradation process for methyl orange solution at acidic condition showed high removal percentage. 5 mg L⁻¹ methyl orange achieved color removal until 94% for 180 min irradiation in photodegradation process with the presence of C-N-codoped TiO₂ catalyst, and approximately 70% TOC removed as the results of mineralization process. The kinetics reaction rate of photodegradation of methyl orange dye with the addition of C-N-codoped TiO₂ followed pseudo-first order represented by Langmuir-Hinshelwood model, the kinetics constant of photodegradation became higher by decreasing the initial concentration of methyl orange. Three organic byproducts of methyl orange formed during photodegradation process was identified by LC-MS/MS system then degradation pathway of methyl orange photodegradation in the presence of C-N-codoped TiO₂ catalyst was proposed.

Keywords: Methyl orange, Photodegradation, C-N-codoped TiO₂, Degradation-pathway

Introduction

The presence of synthetic organic dye in wastewater discharge from textile industries leads to a huge environmental hazard. The wastewater not only causes disruption of aquatic ecosystem because dye-bearing effluents inhibit the penetration of sunlight, but also visually reduces the esthetic quality of water. One of the main pollution from textile wastewater constitute of azo dyes [1]. These dyes have been confirmed to be toxic, mutagenic, and carcinogenic [2-4]. Thus remediation of these dyes from textile wastewater is an imperative research.

Methyl orange (MO), a simple azo dyes, was chosen as an artificial wastewater pollutant in this study. Conventionally, remediation methods for methyl orange such as coagulation [5], flocculation [6] and adsorption using chitosan [7, 8] and activated carbon [9] are currently used. However, these methods only transfer the dye from one phase to another, producing a secondary pollution [10]. Nowadays, photocatalysis have developed as promising solution to solve these pollution problems [11].

Titanium dioxide (TiO₂) is one of the most frequently studied as semiconductor photocatalytic

*Corresponding author e-mail: safni@sci.unand.ac.id

Received 9/07/2019; Accepted 8/10/2019

DOI: 10.21608/ejchem.2019.14543.1883

©2019 National Information and Documentation Center (NIDOC)

material for decomposition of organic compounds, due to its environmental friendly properties, high chemical stability, and relatively low cost [12-14]. Owing to the broad band gap of titania (anatase, ~3.2 eV) there are some disadvantages to its effectiveness in photocatalysis applications [11] such as titania is active only in ultraviolet-light irradiation with high energy [15-17]. Another disadvantages, the high recombination of photo-generated electron-hole pair of titania resulting in low photocatalytic activity and low affinity [18, 19]. Modification of TiO₂ with non-metals dopant such as nitrogen and carbon have been proposed to enhance photocatalytic activity in visible-light irradiation to degrade organic and inorganic pollutant [20-23].

This publication focused on reported the kinetics reaction of methyl orange photodegradation in the presence of C-N-codoped TiO₂ catalyst. To optimize the kinetics model, parameters of photodegradation process were investigated such as C-N-codoped TiO₂ dosage, initial concentration of methyl orange, and initial pH of methyl orange solution. In addition, the transformations of methyl orange molecule during photodegradation process were identified through the analysis of molecular structure by LC-MS/MS system. Then, the possible photodegradation pathway of methyl orange in the presence of C-N-codoped TiO₂ was proposed.

Experimental

Reagents

Methyl orange, MO, (C₁₄H₁₄N₃SO₃Na) ACS grade was purchased from Sigma Aldrich used as model pollutant without further purification. Simulating pollutant solution were prepared by dissolving accurately weighted amount of methyl orange in deionized water (R = 18.2 MΩ cm⁻¹, Milli-Q). Graphite carbon-powder (10 wt.%) were used as the source of carbon dopant and ammonia solution (*Merck*, 25%) as the source of nitrogen dopant. C-N-codoped TiO₂ was prepared from carbon-nitrogen-aqueous peroxotitanate solutions (CN-PTA) using sol-gel organic-free preparation [20, 21].

Characterization

The morphology of C-N-codoped TiO₂ particle was observed with transmission electron microscope (TEM HT7700) and SEM JEOL JSM-6510LA equipped with energy dispersive

X-ray spectroscopy (EDX) for chemical analysis was used. The X-ray diffraction (XRD) patterns of C-N-codoped TiO₂ powder were obtained with Philips X'pert Powder, PANalytical, X-ray diffractometer using Cu-Kα radiation sources (λ = 0.1540 nm).

Photolysis experiment of methyl orange

The photodegradation experiments were performed at room temperature (293 K) and atmospheric pressure inside black irradiation box equipped with a visible-halogen lamp (Phillips, 500 W) as a light source. The distance between lamp and dye solution was kept at 10 cm. For each experiments, the initial concentration of 5 mg L⁻¹ methyl orange was used with the natural pH of methyl orange dye solution was 5.6. The amount of C-N-codoped TiO₂ was 0.4 g L⁻¹ for every photocatalysis and adsorption experiments. Some parameters of photodegradation process were studied such as the effect of C-N-codoped TiO₂ catalyst dosage, the effect of initial dye concentration, the effect of initial pH of methyl orange solution. The photodegradation process of methyl orange was evaluated by monitoring the color removal by HPLC (High Performance Liquid Chromatography) system.

Sample analysis

All aliquotes samples were filtered by 0.45 μm dismic filter (Advantec, Japan) to separate C-N-codoped TiO₂ particles prior to analysis. The methyl orange dye concentration before and after degradation were determined by HPLC using a Summit™ HPLC system (Dionex, USA). A ODS-hypersyl (Thermo Scientific) column (150 mm × 4.6 mm) with 5 μm particle size was used. The mixture solvents of acetonitrile: 0.01 M ammonium acetate (30:70, v/v %) were used as the mobile phase. The detector was performed with visible lamp and was set at 460 nm. The degradation percentage of dye from each solution at different time interval and condition is calculated by Eq. 1:

$$\% \text{ MO removal} = \frac{C_t}{C_0} \times 100\% \quad (1)$$

where C₀ is the initial concentration of methyl orange dyes and C_t is concentration of methyl orange dyes after photolysis process at different condition. The reaction kinetics was evaluated based on the Langmuir-Hinshelwood kinetic model.

By-products analysis

Organic by-products during photocatalysis process as intermediate compounds were measured by LC-MS/MS system. Mass spectra were obtained by direct injection into a mass spectrometer using a Harvard syringe pump (Model 975 Harvard Apparatus, Dover, Mass., USA). The fragmentation of precursor ions was performed to identify product ions using collision energy provided by nitrogen gas. The negative ion mode was then used to scan the entire m/z value from 60 to 400 to obtain fragmentation data of the degradation by-products.

Results and Discussion

Characterization of C-N-codoped TiO_2 catalyst

X-ray diffractometry was used to investigate the crystal identity of TiO_2 samples before and after doping by carbon and nitrogen elements. Figure 1 compares the XRD patterns of the C-N-codoped and undoped TiO_2 . Compared to TiO_2 -anatase standard (ICSD no. 82084), both undoped and C-N-codoped TiO_2 showed anatase crystalline peaks at 2θ values of 25° (101); 37° (004); 48° (200); 54° (105); 55° (211). Thus, doped by carbon and nitrogen elements maintained the anatase phase of TiO_2 crystalline [21]. From diffractogram patterns, C-N-codoped TiO_2 have a clear peak broadening due to the smaller crystalline size of TiO_2 nanoparticles versus to undoped TiO_2 . Based on the calculation of Scherrer formula, the crystalline size of undoped and C-N-codoped TiO_2 were 18 nm and 9 nm, respectively.

Figure 2a-b represents the typical TEM images of TiO_2 particles before and after doped by carbon and nitrogen elements. It can be observed that the aggregation of C-N-codoped TiO_2 particles is more serious than undoped TiO_2 particles. The reason due to carbon species can locate at the surface of TiO_2 particles and act a role of linker between the aggregated particles. The EDX spectra in Fig. 2c confirmed that TiO_2 after doping process contained carbon and nitrogen elements.

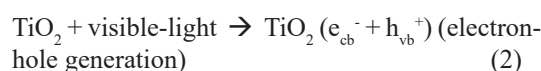
Effect of C-N-codoped TiO_2 catalyst dosage

The effect of C-N-codoped TiO_2 dosage on the photodegradation of methyl orange was investigated in the variation of 0.1 g L^{-1} to 1.0 g L^{-1} . The dye removal results are presented in Fig. 3. It was observed that maximum methyl orange dye removal is achieved in the concentration of 0.45 g L^{-1} C-N-codoped TiO_2 catalyst. The

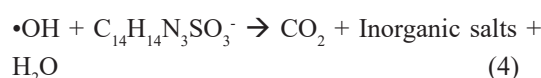
photodegradation of organic pollutant in the presence of catalyst has exhibited the dependency on the catalyst dosage. This can be explained on the increase of catalyst dosage, total active surface area of catalyst increases hence more active sites are available on catalyst surface which resulted in increasing of hydroxyl radicals thus the number of degraded dye molecules increases [24, 25]. However more addition of catalyst may not be useful in photodegradation of methyl orange dye because high dose of catalyst will establish turbidity suspension which cause inhibition in the penetration of visible light [26, 27].

Effect of C-N-codoped TiO_2 in the photocatalysis process

Figure 4 shows the comparison of methyl orange degradation in the process of adsorption, photolysis, and photocatalysis. The adsorption was performed by exposed methyl orange to C-N-codoped TiO_2 in the dark condition. The result shows that only small amount of methyl orange dye (about 5%) was adsorbed on the C-N-codoped TiO_2 surface after 210 minutes. Meanwhile, the photolysis experiment which was performed by exposing methyl orange dye to visible light without the addition of C-N-codoped TiO_2 shows approximately 10% of methyl orange removed. About 96% of methyl orange was removed in photocatalysis process. The dye removal percentage increase significantly in the presence of C-N-codoped TiO_2 due to the more highly reactive species, hydroxyl radicals ($\bullet OH$), were produced. The hydroxyl radical will react to methyl orange dye molecules and achieve mineralization process. During visible-light penetration to C-N-codoped TiO_2 , the hydroxyl radical was produced by the reaction between electron vacancy or hole site (h^+) of TiO_2 with water molecules [28, 29]. The reaction was shown at Eq. (2-3):



Then, hydroxyl radicals attack the organic molecule of methyl orange producing inorganic salts and hydrogen dioxide [30, 31]. The reaction was shown at Eq. 4:



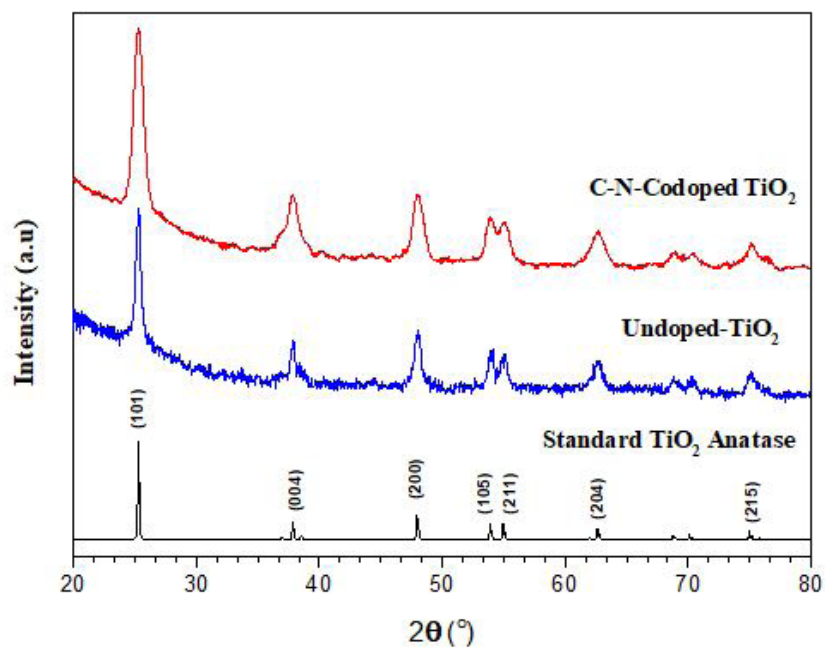
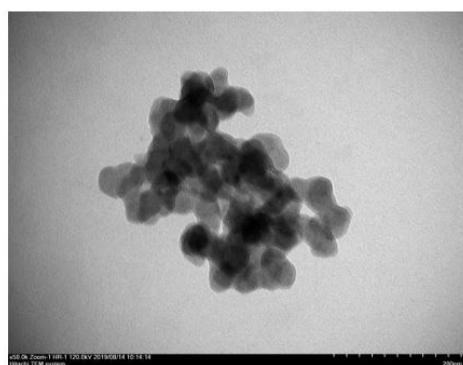
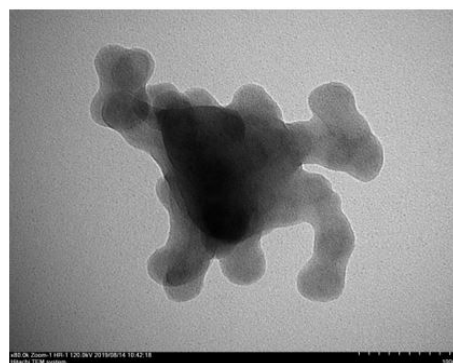


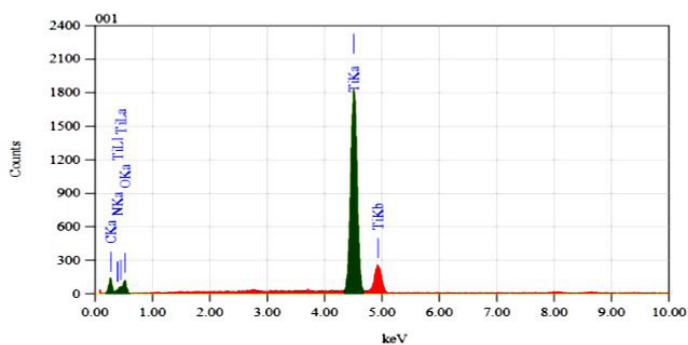
Fig. 1. The comparison XRD patterns of C-N-codoped TiO_2 ; undoped- TiO_2 ; and standard TiO_2 -anatase



(a)



(b)



(c)

Elements	Atom (%)
Ti	39.6
O	41.79
C	16.59
N	2.02

Fig. 2. TEM image (a) undoped- TiO_2 and (b) C-N-codoped TiO_2 ; (c) EDX spectrum of C-N-codoped TiO_2

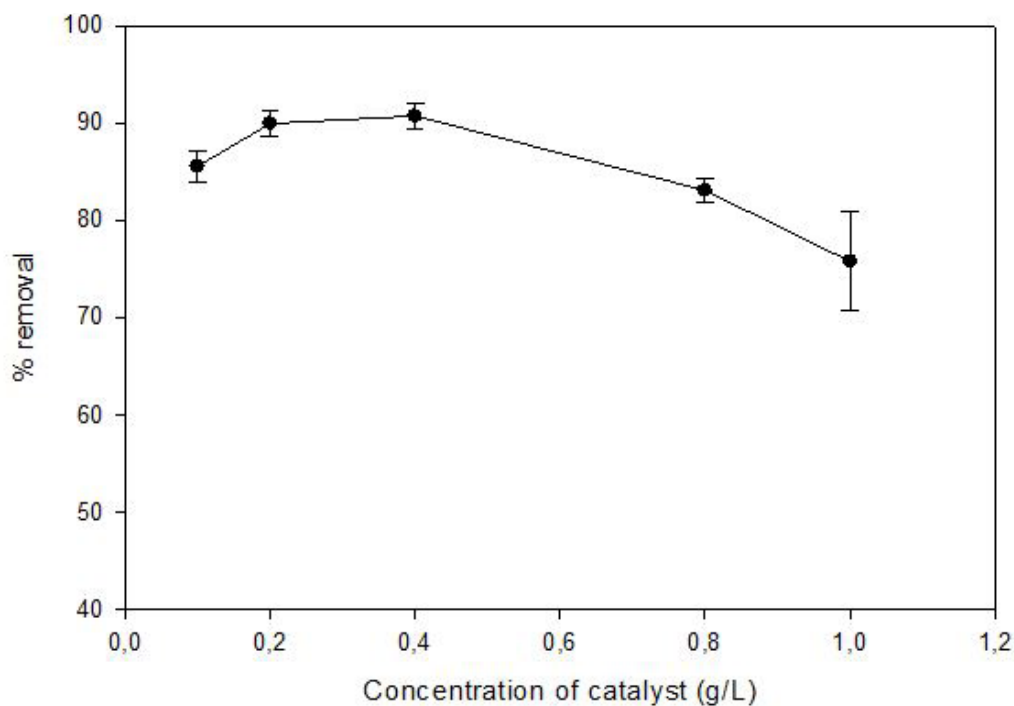


Fig. 3. Effect of C-N-codoped TiO_2 dosage in the photodegradation for 180 min. (MO = 5 mg L^{-1} ; pH = 5.6; $n=2$) n : number of sample size

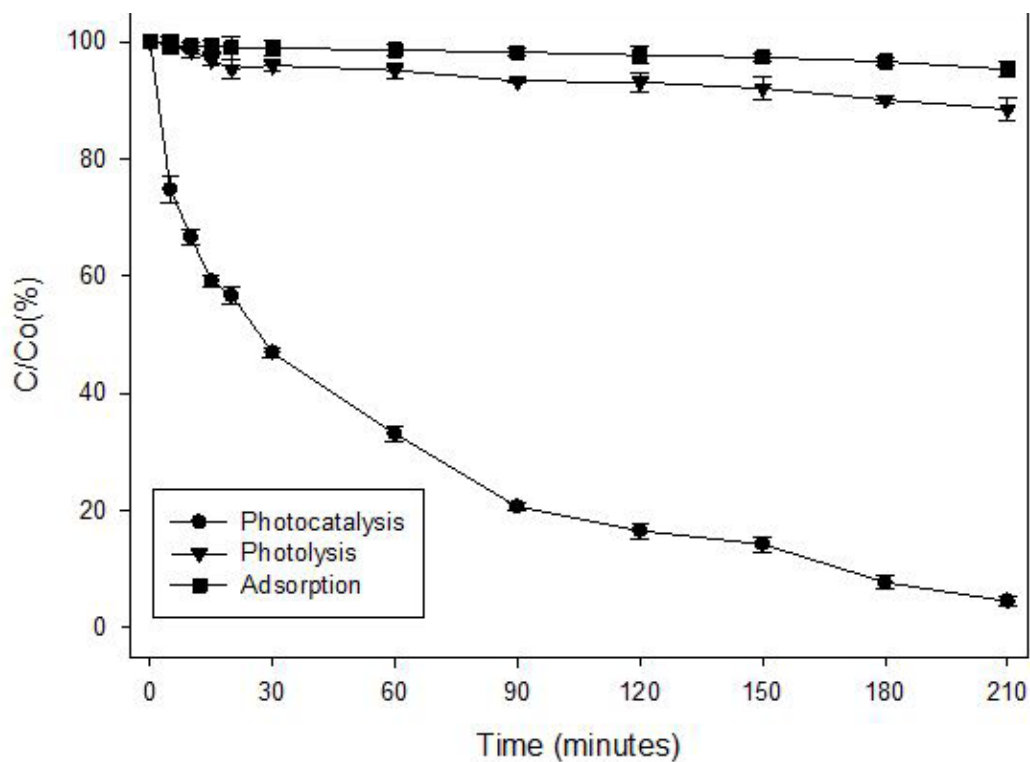


Fig. 4. Comparison of adsorption, photolysis, and photocatalysis in degradation of methyl orange (MO = 5 mg L^{-1} ; pH = 5.6; $n=2$)

Effect of initial methyl orange concentration

The degradation of different methyl orange initial concentrations were studied, the results are shown in Fig. 5. It has been found that the color removal efficiency of methyl orange was decreased with increasing the initial concentration of methyl orange dye. High concentration of methyl orange causes declining transparency of the solution thus penetration of visible light to organic molecules of methyl orange dye decreased [32, 33]. Therefore, the time to complete removal of methyl orange dye longer for higher initial dye concentration.

Study of Kinetic Order

The Langmuir-Hinshelwood kinetic model can be applied for photodegradation of methyl orange in the presence of C-N-codoped TiO₂ catalyst in the correlation between the degradation rate and the initial dye concentration [34]. In this research the initial concentrations of methyl orange dye used were relatively low, hence the kinetics data were modelled using pseudo first-order. The kinetics can be expressed by the following formula:

$$C = C_0 e^{-k t} \quad (5)$$

where C is the concentration of methyl orange at time t, C₀ is the initial concentration of methyl orange and k (min⁻¹) is the degradation rate constant. The integration of Eq. 5 results in Eq. 6:

$$\ln\left(\frac{C}{C_0}\right) = -k t \quad (6)$$

Based on Eq. 6, a plot of ln(C/C₀) versus irradiation time represents a straight line showing in Fig. 6. The value of methyl orange degradation rate constant at each concentration was shown in Table 1. From the pseudo-first-order constant, the contribution of adsorption and oxidation in the photodegradation of methyl orange could be estimated by the equation of Langmuir-Hinshelwood model [35, 36], Eq. 7:

$$\frac{1}{k} = \frac{1}{K_{MO} k_{rxn}} + \frac{C_0}{k_{rxn}} \quad (7)$$

where K_{MO} (L mg⁻¹) is equilibrium adsorption constant of methyl orange on C-N-codoped TiO₂ and k_{rxn} (mg L⁻¹ min⁻¹) is the reaction rate between methyl orange and •OH radicals.

As shown in Fig. 7, the degradation rate constant of pseudo first-order for photodegradation of methyl orange at various initial concentration in the presence of C-N-codoped TiO₂ was fitted to Eq. 7. The resulting values of k_{rxn} and K_{MO} obtained were 0.236 mg L⁻¹ min⁻¹ and 10.436 L mg⁻¹ with the R² value of 0.9142, respectively.

Egypt. J. Chem. **62**, Special Issue (Part 2) (2019)

Effect of initial pH methyl orange solution

The effect of pH on methyl orange photodegradation was investigated in the presence of C-N-codoped TiO₂ catalyst. The acidic condition was made by the addition of HCl (0.1 M) and base condition by the addition of NaOH (0.1 M). The results obtained in the pH range 3-9 are shown in Fig. 8. It was observed that the best degradation efficiency was obtained at pH 3.6. It is known that TiO₂ has amphoteric character in aqueous solution. The point of zero charge (p_{zc}) of C-N-codoped TiO₂ was found at acidic pH (5.29) [37]. Since the pH condition of dye solution near the p_{zc} can be favorable to adsorb the molecule of methyl orange and therefore the highest degradation percentage was achieved at pH 3.6. Base pH condition decreased the degradation efficiency due to the coulombic repulsion between negative charge of catalyst surface (TiO₂⁻) at alkaline condition [38] and the OH⁻ species in photocatalytic mechanism [35]. The degradation percentage at natural pH of methyl orange (5.6) was slightly different to acidic pH thus this pH was chosen for investigation of kinetics reaction since no need HCl addition.

Byproducts analysis and photodegradation mechanism

To confirm the mineralization process in the photodegradation of methyl orange using C-N-codoped TiO₂ catalyst, the reaction were carried out up to 180 min and the irradiated samples were analyzed by TOC (Total Organic Carbon) analyzer. The TOC-removal percentage of methyl orange gradually increased with time. After 180 min reaction, the TOC-removal percentage reached approximately 70%, the results are shown in Fig. 9. However, compared with the color removal of methyl orange, the removal percentage of TOC was slightly lower under the same conditions. This occurred mainly because the methyl orange macromolecule broke into an organic small molecular substances and was finally oxidized to form an inorganic substance (CO₂) during the photocatalytic degradation of MO. The small molecular substances were detected in the analysis of HPLC system. Fig. 10 shown the chromatogram of methyl orange during photodegradation process for 180 min. Some peaks were indicated as by-products of methyl orange then identified by LC-MS/MS system.

As seen from Fig. 10a, methyl orange has a strong peak at retention time RT 4.120 min. After photodegradation process for 180 min the peak significantly decreased and some peaks were formed indicating as byproducts (in Fig. 10b-e). The peaks were identified in MS/MS system then known as organic compounds with m/z 290; 158; and 123. Other small peak at 120 min degradation was also identified with m/z 276. After 180 min degradation the organic structure with m/z 276 was not showed up and transferred into other molecules. Hence, the tentative molecular structure and proposed pathway for methyl orange photodegradation in the presence of C-N-codoped TiO₂ are shown in Fig. 11.

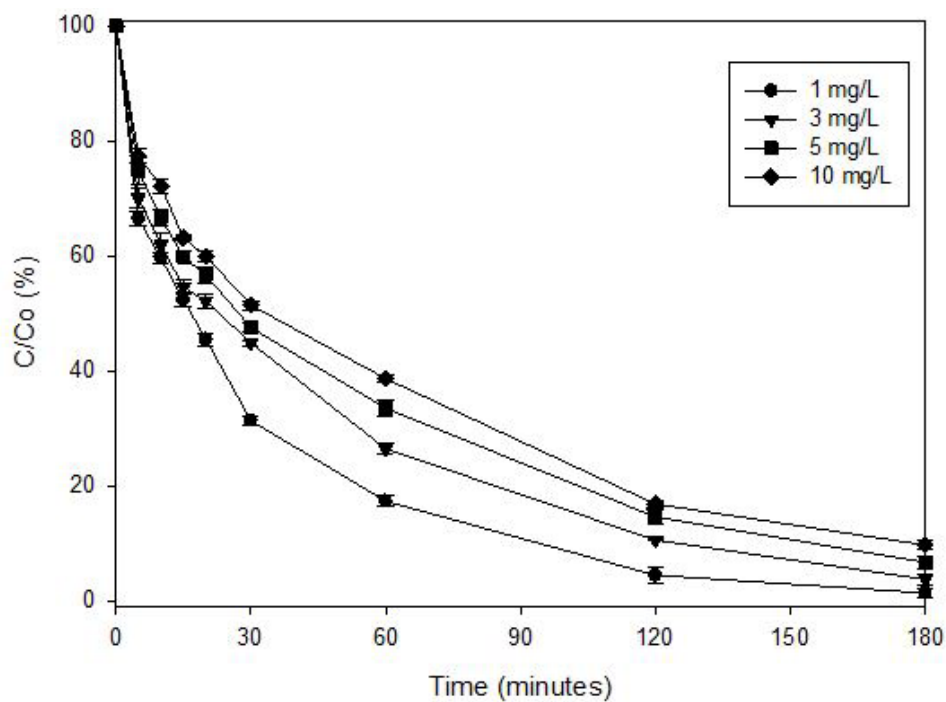


Fig. 5. Effect of methyl orange initial concentration to color removal ($C-N$ -codoped $TiO_2 = 0.45 \text{ g L}^{-1}$; $pH = 5.6$; $n=2$)

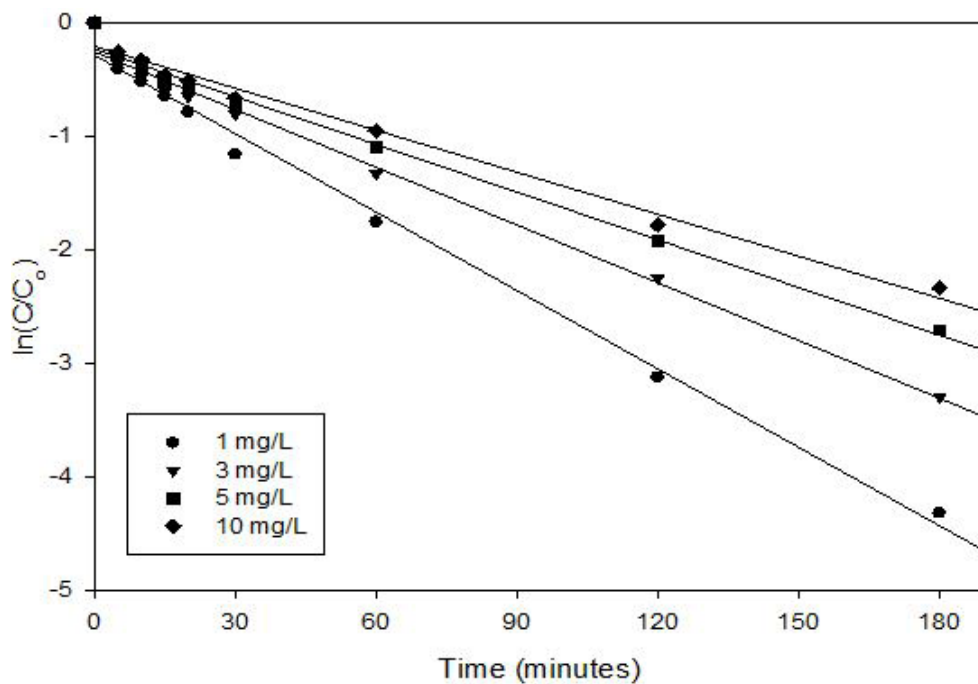


Fig. 6. Photodegradation kinetics model in various concentration of methyl orange in the present of catalyst ($pH = 5.6$, $C-N$ -codoped $TiO_2 = 0.45 \text{ g L}^{-1}$, $n=2$)

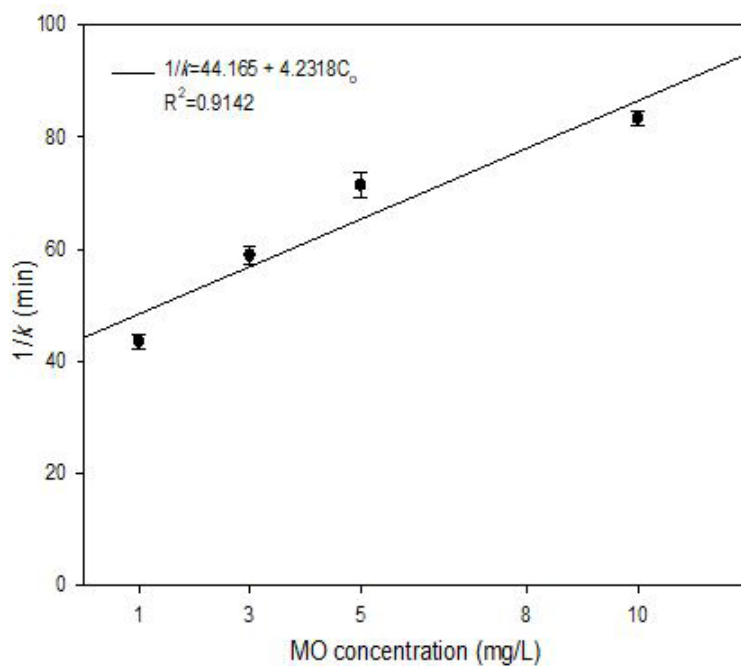


Fig. 7. Plot of the initial MO concentration versus the reciprocal of pseudo-first-order rate constant (1/k)

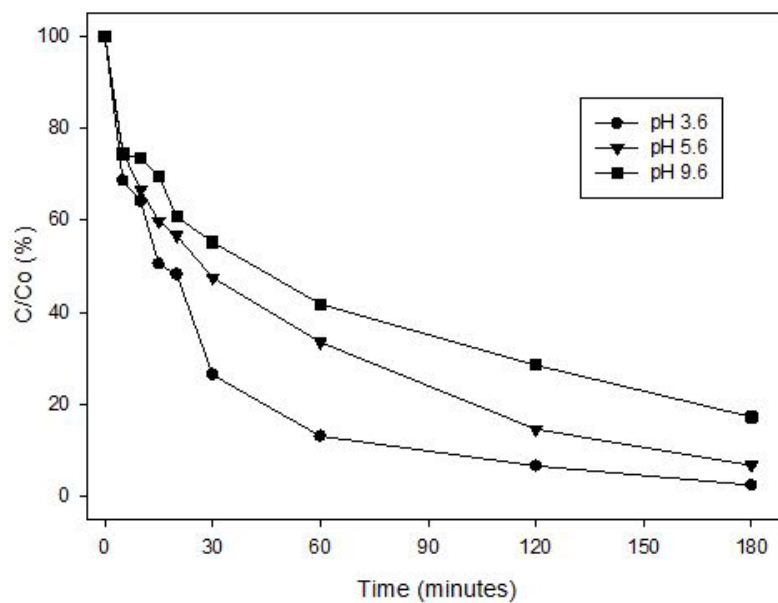


Fig. 8. Effect of methyl orange initial pH to color removal (MO= 5 mg L⁻¹; C-N-codoped TiO₂= 0.45 g L⁻¹; n=2)

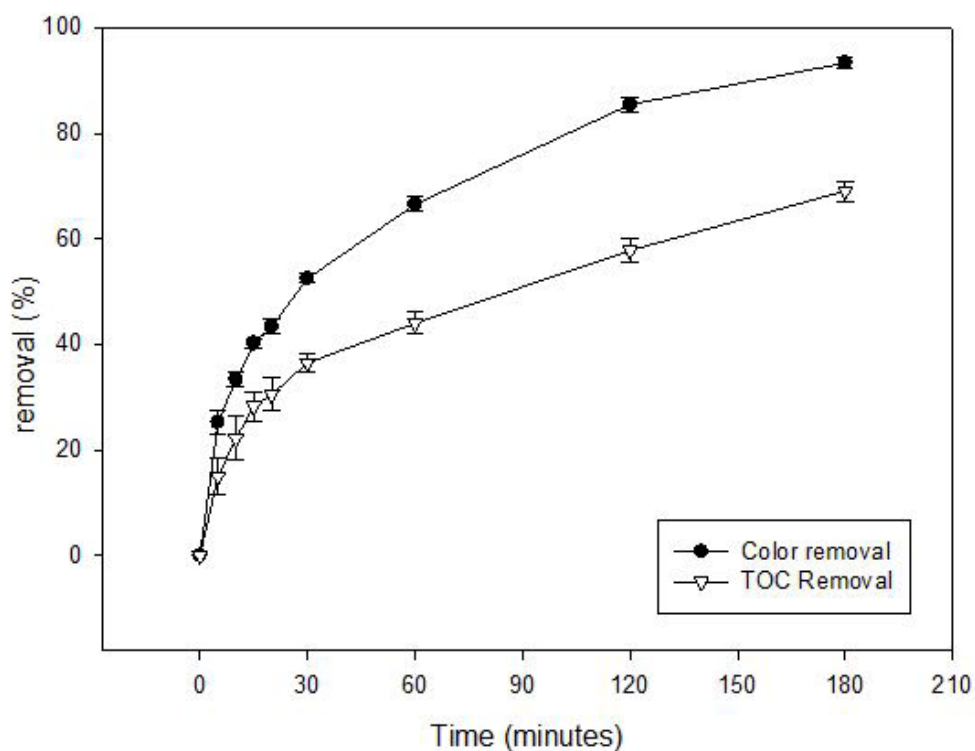


Fig. 9. Color and TOC removal comparison of methyl orange during photodegradation (MO= 5 mg L⁻¹; C-N-codoped TiO₂= 0.45 g L⁻¹; pH= 5.6; n=2)

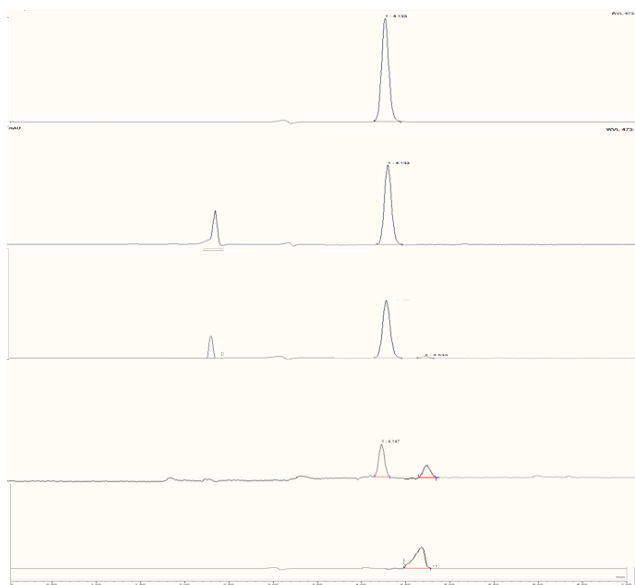


Fig. 10. chromatogram of methyl orange during photodegradation for (a) 0 min;(b) 30 min;(c) 60 min;(d) 120 min;(e) 180 min). (MO= 5 mg L⁻¹; C-N-codoped TiO₂= 0.45 g L⁻¹; pH= 5.6)

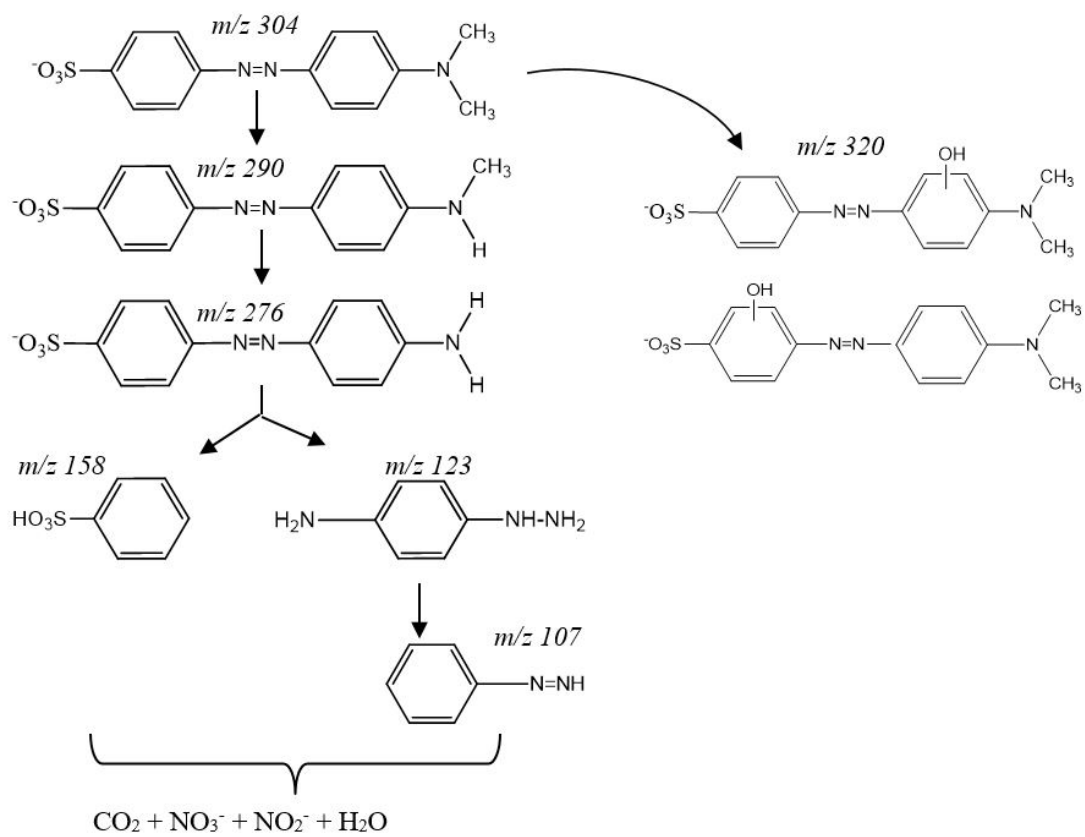


Fig. 11. Schematic illustration of the proposed degradation pathway

TABLE 1. Methyl orange degradation rate based on Langmuir-Hinshelwood model (experimental conditions: mass of C-N-codoped $TiO_2 = 0.45 \text{ g L}^{-1}$, $pH=5.6$, $n=2$)

Initial dye(mg L^{-1})	k_{obs} (min^{-1})	$1/k_{\text{obs}}$ (min)	$t_{1/2}$ (min)	R^2
1	0.023	43.41	30.09	0.9912
3	0.017	58.94	40.86	0.9901
5	0.014	71.38	49.47	0.9877
10	0.012	81.01	56.15	0.9839

Conclusion

The experimental results of this study show that photo-degradation using C-N-codoped TiO₂ as a catalyst could be applied to the treatment of methyl orange wastewater. About 4% of methyl orange was adsorbed onto C-N-codoped TiO₂ surface, and 10% of methyl orange was degraded during photodegradation then by the addition of 0.45 g L⁻¹ of C-N-codoped TiO₂ the color removal of methyl orange increase to 94% for 180 min visible-light irradiation. The photodegradation of methyl orange using C-N-codoped TiO₂ catalyst was fitted to the Langmuir-Hinshelwood model and obeyed the pseudo-first-order kinetics. In the mineralization study, the photolysis process in the presence of C-N-codoped TiO₂ achieved an approximately 70% TOC removal. The organic byproducts were identified by LC-MS/MS system then the degradation pathway of methyl orange was proposed.

Acknowledgement

The authors would like to acknowledge the support of the Ministry of Research, Technology and Higher Education of Republic of Indonesia (RISTEKDIKTI). This research was fully supported by the master program of education leading to doctoral degree for excellent graduates (PMDSU) (Grant No. 050 / SP2H / LT / DRPM / 2018).

References

1. Kaur, J. and S. Singhal, Facile synthesis of ZnO and transition metal doped ZnO nanoparticles for the photocatalytic degradation of Methyl Orange. *Ceramics International*, **40** (5), 7417-7424 (2014).
2. Chung, K.-T., Azo dyes and human health: A Review. *J. Environ. Sci. Health C Environ. Carcinog. Ecotoxicol. Rev.*, **34** (4), 233-261 (2016).
3. Cox, J.A. and P.A. White, The mutagenic activity of select azo compounds in MutaMouse target tissues in vivo and primary hepatocytes in vitro. *Mutat Res Gen Tox En*, **844**, 25-34 (2019).
4. Gičević, A., L. Hindija, and A. Karačić, Toxicity of Azo Dyes in Pharmaceutical Industry. *International Conference on Medical and Biological Engineering*, **73**, 581-587 (2020).
5. Yen-Yie Lau, Y.-S.W.T.-T.T., Norhashimah Morad, and S.-A.O. Mohd Rafatullaha, Degradation of cationic and anionic dyes in coagulation-flocculation process using bi-functionalized silica hybrid with aluminum-ferric as auxiliary agent *RSC Advances*, **5**, 34206-34215 (2015).
6. Habiba, U., T.A. Siddique, T.C. Joo, A. Salleh, B.C. Ang, and A.M. Affi, Synthesis of chitosan/polyvinyl alcohol/zeolite composite for removal of methyl orange, Congo red and chromium(VI) by flocculation/adsorption. *Carbohydr Polym*, **157**, 1568-1576 (2017).
7. Huang, R., Q. Liu, J. Huo, and B. Yang, Adsorption of methyl orange onto protonated cross-linked chitosan. *Arabian Journal of Chemistry*, **10** (1), 24-32 (2017).
8. Zhai, L., Z. Bai, Y. Zhu, B. Wang, and W. Luo, Fabrication of chitosan microspheres for efficient adsorption of methyl orange. *Chinese Journal of Chemical Engineering*, **26** (3), 657-666 (2018).
9. Mahmoudi, K., K. Hosni, N. Hamdi, and E. Srasra, Kinetics and equilibrium studies on removal of methylene blue and methyl orange by adsorption onto activated carbon prepared from date pits-A comparative study. *Korean Journal of Chemical Engineering*, **32** (2), 274-283 (2014).
10. El Fawal, G., A. Ibrahim, and M. Akl, Methylene blue and crystal violet dyes removal (as a binary system) from aqueous solution using local soil clay: kinetics study and equilibrium isotherms. *Egyptian Journal of Chemistry*, **62** (3), 941-954 (2018).
11. Nguyen, C.H., C.-C. Fu, and R.-S. Juang, Degradation of methylene blue and methyl orange *Egypt.J.Chem.* **62**, Special Issue (Part 2) (2019)

- by palladium-doped TiO₂ photocatalysis for water reuse: Efficiency and degradation pathways. *Journal of Cleaner Production*, **202**, 413-427 (2018).
12. Thompson, T.L. and J. John T. Yates, Surface science studies of the photoactivation of TiO₂-new photochemical process. *Chem. Rev*, **106**, 4428-4453 (2006).
 13. Gholamreza Moussavi, M.B., Mahdi Farzadkia, Roghieh Ahmadi Asl, Decolorization and mineralization of Reactive Red 198 in saline water: Performance comparison of photolysis UV/TiO₂ and UV/ZnO processes. *Environmental Engineering and Management Journal*, **14** (5), 1027-1036 (2015).
 14. Phutthamon Chantes, Chalor Jarusutthirak, and S. Danwittayakul, A Comparison Study of Photocatalytic Activity of TiO₂ and ZnO on the Degradation of Real Batik Wastewater. *International Conference on Biological, Environment and Food Engineering*, 8-12 (2015).
 15. Joseph, C.G., Y.H. Taufiq-Yap, G. Li Puma, K. Sanmugam, and K.S. Quek, Photocatalytic degradation of cationic dye simulated wastewater using four radiation sources, UVA, UVB, UVC and solar lamp of identical power output. *Desalination and Water Treatment*, **57** (17), 7976-7987 (2015).
 16. Kordouli, E., K. Bourikas, A. Lycourghiotis, and C. Kordulis, The mechanism of azo-dyes adsorption on the titanium dioxide surface and their photocatalytic degradation over samples with various anatase/rutile ratios. *Catalysis Today*, **252**, 128-135 (2015).
 17. Dariani, R.S., A. Esmaili, A. Mortezaali, and S. Dehghanpour, Photocatalytic reaction and degradation of methylene blue on TiO₂ nano-sized particles. *Optik*, **127** (18), 7143-7154 (2016).
 18. Kerkez-Kuyumcu, Ö., E. Kibar, K. Dayioğlu, F. Gedik, A.N. Akın, and Ş. Özkara-Aydinoğlu, A comparative study for removal of different dyes over M/TiO₂ (M = Cu, Ni, Co, Fe, Mn and Cr) photocatalysts under visible light irradiation. *Journal of Photochemistry and Photobiology A: Chemistry*, **311**, 176-185 (2015).
 19. Długokęcka, M., J. Łuczak, Ż. Polkowska, and A. Zaleska-Medynska, The effect of microemulsion composition on the morphology of Pd nanoparticles deposited at the surface of TiO₂ and photoactivity of Pd-TiO₂. *Applied Surface Science*, **405**, 220-230 (2017).
 20. Xu, Q.C., D.V. Wellia, S. Yan, D.W. Liao, T.M. Lim, and T.T. Tan, Enhanced photocatalytic activity of C-N-codoped TiO₂ films prepared via an organic-free approach. *J Hazard Mater*, **188** (1-3), 172-80 (2011).
 21. Wellia, D.V., D. Fitria, and S. Safni, C-N-Codoped TiO₂ Synthesis by using Peroxo Sol Gel Method for Photocatalytic Reduction of Cr(VI). *The Journal of Pure and Applied Chemistry Research*, **7** (1), 26-32 (2018).
 22. Safni, D.V. Wellia, P.S. Komala, and R.A. Putri, Degradation of yellow-GCN by photolysis with UV-light and irradiation using C-N-codoped TiO₂ catalyst. *J. Chem. Pharm. Res.*, **7** (11), 306-311 (2015).
 23. Safni, R.A. Putri, D.V. Wellia, and U. Septiani, Photodegradation of Orange F3R dyes effect of light sources and the addition of C-N-Codoped TiO₂ catalyst. *Der Pharma Chemica*, **9** (10), 1-5 (2017).
 24. Naraginti, S., F.B. Stephen, A. Radhakrishnan, and A. Sivakumar, Zirconium and silver co-doped TiO₂ nanoparticles as visible light catalyst for reduction of 4-nitrophenol, degradation of methyl orange and methylene blue. *Spectrochim Acta A Mol Biomol Spectrosc*, **135**, 814-9 (2015).
 25. Abd Rahman, N., M.S. Azami, W.I. Nawawi, M.A.M. Ishak, K. Ismail, Z. Ahmad, A.H. Jawad, Z. Mohd Jaini, R. Yunus, and S.N. Rahmat, Carbon Nitrogen Co-Doped P25: Parameter Study on Photodegradation of Reactive Red 4. *MATEC Web of Conferences*, **47**, 05018 (2016).
 26. Kaur, N., S. Kaur, and V. Singh, Preparation, characterization and photocatalytic degradation kinetics of Reactive Red dye 198 using N, Fe codoped TiO₂ nanoparticles under visible light. *Desalination and Water Treatment*, **57** (20), 9237-9246 (2015).
 27. Bai, L., S. Wang, Z. Wang, E. Hong, Y. Wang, C. Xia, and B. Wang, Kinetics and mechanism of photocatalytic degradation of methyl orange in water by mesoporous Nd-TiO₂-SBA-15 nanocatalyst. *Environ Pollut*, **248**, 516-525 (2019).
 28. Rauf, M.A., M.A. Meentani, and S. Hisaindee, An overview on the photocatalytic degradation of azo dyes in the presence of TiO₂ doped with selective transition metals. *Desalination*, **276** (1-3), 13-27 (2011).
 29. Ananpattarachai, J., S. Seraphin, and P. Kajitvichyanukul, Formation of hydroxyl radicals and kinetic study of 2-chlorophenol photocatalytic oxidation using C-doped TiO₂, N-doped TiO₂, and C,N Co-doped TiO₂ under visible light. *Environ Sci Pollut Res Int*, **23** (4), 3884-96 (2016).
 30. He, Z., W. Que, J. Chen, X. Yin, Y. He, and J. Ren, Photocatalytic degradation of methyl orange
- Egypt.J.Chem.* **62**, Special Issue (Part 2) (2019)

- over nitrogen-fluorine codoped TiO₂ nanobelts prepared by solvothermal synthesis. *ACS Appl Mater Interfaces*, **4** (12), 6816-6826 (2012).
31. Lu, L., R. Shan, Y. Shi, S. Wang, and H. Yuan, A novel TiO₂/biochar composite catalysts for photocatalytic degradation of methyl orange. *Chemosphere*, **222**, 391-398 (2019).
 32. Youssef, N.A., S.A. Shaban, F.A. Ibrahim, and A.S. Mahmoud, Degradation of methyl orange using Fenton catalytic reaction. *Egyptian Journal of Petroleum*, **25** (3), 317-321 (2016).
 33. Seifhosseini, M., F. Rashidi, M. Rezaei, and N. Rahimpour, Bias potential role in degradation of methyl orange in photocatalytic process. *Journal of Photochemistry and Photobiology A: Chemistry*, **360**, 196-203 (2018).
 34. Saïen, J. and Z. Mesgari, Photocatalytic degradation of methyl orange using hematoporphyrin/N-doped TiO₂ nano hybrids under visible light: Kinetics and energy consumption. *Applied Organometallic Chemistry*, **31** (11), 1-11 (2017).
 35. Son, H.S., S.J. Lee, I.H. Cho, and K.D. Zoh, Kinetics and mechanism of TNT degradation in TiO₂ photocatalysis. *Chemosphere*, **57** (4), 309-17 (2004).
 36. Son, H.S., G. Ko, and K.D. Zoh, Kinetics and mechanism of photolysis and TiO₂ photocatalysis of triclosan. *J Hazard Mater*, **166** (2-3), 954-60 (2009).
 37. Wang, X. and T.-T. Lim, Solvothermal synthesis of C-N codoped TiO₂ and photocatalytic evaluation for bisphenol A degradation using a visible-light irradiated LED photoreactor. *Applied Catalysis B: Environmental*, **100** (1-2), 355-364 (2010).
 38. Liu, J., R. Han, Y. Zhao, H. Wang, W. Lu, T. Yu, and Y. Zhang, Enhanced photoactivity of V-N Codoped TiO₂ derived from a two-step hydrothermal procedure for the degradation of PCP-Na under visible light irradiation. *The Journal of Physical Chemistry C*, **115** (11), 4507-4515 (2011).